Article

Potent and Selective Structure-Based Dibenzofuran Inhibitors of Transthyretin Amyloidogenesis: Kinetic Stabilization of the Native State

H. Michael Petrassi, Steven M. Johnson, Hans E. Purkey, Kyle P. Chiang, Traci Walkup, Xin Jiang, Evan T. Powers, and Jeffery W. Kelly

J. Am. Chem. Soc., **2005**, 127 (18), 6662-6671• DOI: 10.1021/ja044351f • Publication Date (Web): 15 April 2005

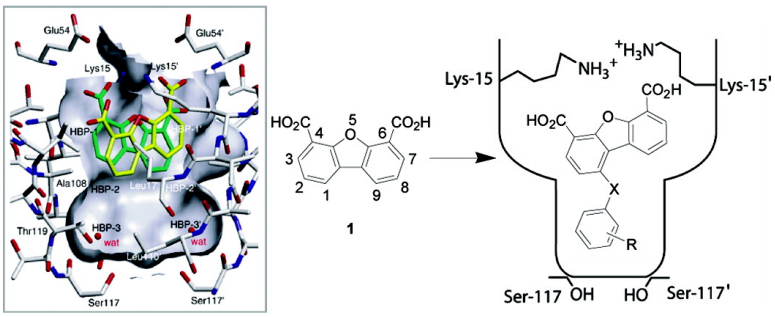

More About This Article

Additional resources and features associated with this article are available within the HTML version:

- Supporting Information
- Links to the 4 articles that cite this article, as of the time of this article download
- Access to high resolution figures
- Links to articles and content related to this article
- Copyright permission to reproduce figures and/or text from this article

View the Full Text HTML

J|A|C|S
ARTICLES
Published on Web 04/15/2005

Potent and Selective Structure-Based Dibenzofuran Inhibitors of Transthyretin Amyloidogenesis: Kinetic Stabilization of the Native State

H. Michael Petrassi, Steven M. Johnson, Hans E. Purkey, Kyle P. Chiang, Traci Walkup, Xin Jiang, Evan T. Powers, and Jeffery W. Kelly*

Contribution from the Department of Chemistry and The Skaggs Institute of Chemical Biology, The Scripps Research Institute, 10550 North Torrey Pines Road, BCC265, La Jolla, California 92037

Received September 16, 2004; E-mail: jkelly@scripps.edu.

Abstract: Transthyretin (TTR) amyloidogenesis requires rate-limiting tetramer dissociation and partial monomer denaturation to produce a misassembly competent species. This process has been followed by turbidity to identify transthyretin amyloidogenesis inhibitors including dibenzofuran-4,6-dicarboxylic acid (**1**). An X-ray cocrystal structure of TTR·$\mathbf{1}_2$ reveals that it only utilizes the outer portion of the two thyroxine binding pockets to bind to and inhibit TTR amyloidogenesis. Herein, structure-based design was employed to append aryl substituents at C1 of the dibenzofuran ring to complement the unused inner portion of the thyroxine binding pockets. Twenty-eight amyloidogenesis inhibitors of increased potency and dramatically increased plasma TTR binding selectivity resulted. These function by imposing kinetic stabilization on the native tetrameric structure of TTR, creating a barrier that is insurmountable under physiological conditions. Since kinetic stabilization of the TTR native state by interallelic trans suppression is known to ameliorate disease, there is reason to be optimistic that the dibenzofuran-based inhibitors will do the same. Preventing the onset of amyloidogenesis is the most conservative strategy to intervene clinically, as it remains unclear which of the TTR misassembly intermediates results in toxicity. The exceptional binding selectivity enables these inhibitors to occupy the thyroxine binding site(s) in a complex biological fluid such as blood plasma, required for inhibition of amyloidogenesis in humans. It is now established that the dibenzofuran-based amyloidogenesis inhibitors have high selectivity, affinity, and efficacy and are thus excellent candidates for further pharmacologic evaluation.

Introduction

Amyloid formation from numerous, nearly identical transthyretin (TTR) sequences appears to cause the organ dysfunction and/or neurodegeneration characteristic of several amyloid diseases.[1−3] In senile systemic amyloidosis (SSA), the amyloid and related aggregates derived from wild-type (WT) TTR lead to cardiac dysfunction, affecting as much as 10% of the human population over age 80.[2] Familial amyloid cardiomyopathy (FAC) is associated with V122I TTR amyloidogenesis in 3−4% of African Americans, ultimately leading to congestive heart failure.[1,4] In familial amyloid polyneuropathy (FAP), one of over 100 TTR variants (e.g., V30M) primarily deposits in and leads to dysfunction of the peripheral nervous system.[5−7] Recently, a few TTR variants that are primarily associated with central nervous system degeneration have also been discovered.[8−10]

There is no effective treatment available today for SSA or FAC. FAP has been successfully treated by liver transplantation, which is a crude form of gene therapy wherein the mutant gene is replaced by a wild-type TTR gene in the liver, which appears to be the main secretory organ for plasma TTR.[11−14] However, liver transplantation requires invasive surgery, an appropriate donor, and the need for sustained immunosuppression; in addition, this therapy is imperfect because WT-TTR continues to deposit in the heart.[15,16] Moreover, recent evidence suggests that this procedure is more effective for V30M heterozygotes

(1) Jacobson, D. R.; Pastore, R. D.; Yaghoubian, R.; Kane, I.; Gallo, G. Buck, F. S.; Buxbaum, J. N. *New Eng. J. Med.* **1997**, *336*, 466−473.
(2) Westermark, P.; Sletten, K.; Johansson, B.; Cornwell, G. G., III. *Proc. Natl. Acad. Sci. U.S.A.* **1990**, *87*, 2843−2845.
(3) Saraiva, M. J.; Sousa, M. M.; Cardoso, I.; Fernandes, R. *J. Mol. Neurosci.* **2004**, *23*, 35−40.
(4) Afolabi, I.; Hamidi, A. K.; Nakamura, M.; Jacobs, P.; Hendrie, H.; Benson, M. D. *Amyloid* **2000**, *7*, 121−125.
(5) Coelho, T. *Curr. Opin. Neurology* **1996**, *9*, 355−359.
(6) Saraiva, M. J. M. *Human Mutat.* **1995**, *5*, 191−196.
(7) Suhr, O. B.; Svendsen, I. H.; Andersson, R.; Danielsson, A.; Holmgren, G. *J. Int. Med.* **2003**, *254*, 225−235.
(8) Hammarstrom, P.; Sekijima, Y.; White, J. P.; Wiseman, R. L.; Lim, A.; Costello, C. E.; Altland, K.; Garzuly, F.; Budka, H.; Kelly, J. W. *Biochemistry* **2003**, *42*, 6656−6663.
(9) Sekijima, Y.; Hammarstrom, P.; Matsumura, M.; Shimizu, Y.; Iwata, M.; Tokuda, T.; Ikeda, S.-I.; Kelly, J. W. *Lab. Invest.* **2003**, *83*, 409−417.
(10) Vidal, R.; Garzuly, F.; Budka, H.; Lalowski, M.; Linke, R. P.; Brittig, F.; Frangione, B.; Wisniewski, T. *Am. J. Pathol.* **1996**, *148*, 361−366.
(11) Herlenius, G.; Wilczek, H. E.; Larsson, M.; Ericzon, B.-G. *Transplantation* **2004**, *77*, 64−71.
(12) Holmgren, G.; Ericzon, B. G.; Groth, C. G.; Steen, L.; Suhr, O. Clinical improvement and amyloid regression after liver transplantation in hereditary transthyretin amyloidosis; Department of Clinical Genetics, University Hospital, Umea, Sweden, United Kingdom, 1993; pp 1113−1116.
(13) Jonsen, E.; Suhr, O. B.; Tashima, K.; Athlin, E. *Amyloid* **2001**, *8*, 52−57.
(14) Suhr, O. B.; Ericzon, B.-G.; Friman, S. *Liver transplantation: official publication of the American Association for the Study of Liver Diseases and the International Liver Transplantation Society* **2002**, *8*, 787−794.

10.1021/ja044351f CCC: $30.25

than for carriers of other FAP mutations for reasons that remain unclear but that may relate to synthesis of TTR by other organs and tissues in the periphery.[17]

Transthyretin serves as a transporter of both thyroid hormone (i.e., thyroxine, T_4) and *holo*-retinol binding protein in the blood and cerebrospinal fluid.[18−21] The extent of TTR aggregation does not appear to be substantial enough to significantly compromise normal function; however, the structure of this protein is integrally associated with its pathology. TTR is a homotetramer composed of 127-residue β-sheet-rich subunits.[18] Amyloid formation occurs by rate-limiting tetramer dissociation, followed by partial monomer denaturation, rendering the protein misassembly competent.[22−28] Numerous aggregates are formed under partial denaturing conditions including amorphous aggregates, soluble cross-β-sheet aggregates and insoluble amyloid fibrils, of which the nonfibrous deposits appear to mediate toxicity.[28,29]

Interallelic trans suppression of FAP has been demonstrated in a Portuguese family who are known to have the highly penetrant V30M disease-associated mutation, yet these individuals do not present with amyloidosis because they have a T119M mutation on their other TTR allele.[30,31] Trans suppression is accomplished by the incorporation of T119M subunits into TTR tetramers otherwise composed of V30M subunits, imparting kinetic stabilization on the native tetrameric state of TTR, preventing amyloidogenesis.[31,32] Incorporation of T119M subunits into the tetramers of these compound heterozygotic individuals raises the activation barrier for tetramer dissociation, dramatically slowing the rate-limiting step of TTR amyloidogenesis and thereby preventing the onset of FAP.[31,32]

The transthyretin homotetramer has 222-symmetry and features a pair of funnel-shaped thyroid hormone (thyroxine) binding sites bisected by the crystallographic C_2 axis.[18,33] Ligand binding to one or both of the TTR thyroxine binding sites imparts kinetic stabilization on the TTR tetramer, a feat that is accomplished by selectively stabilizing the ground state over the dissociative transition state under amyloidogenic conditions.[31,34] High-affinity native state binders raise the kinetic barrier for tetramer dissociation, making it insurmountable under physiological conditions. This is highly desirable as it prevents the process of amyloidogenesis from commencing.[35] Greater than 99% of the TTR thyroxine binding sites are unoccupied because TTR is the tertiary carrier, providing the opportunity to use ligands that selectively bind at one or both of these sites to stabilize TTR in blood. On the basis of the mechanistic analogies with interallelic trans suppression, which is known to ameliorate human disease, there is good reason to believe that a small molecule that selectively binds the native tetrameric state of TTR and imparts kinetic stabilization will be effective at preventing amyloidosis in humans.[31]

Several structurally distinct classes of small molecule TTR amyloidogenesis inhibitors have been discovered, of which dibenzofuran-4,6-dicarboxylic acid (**1**) is particularly interesting, Figure 1.[31,33,34,36−46] This inhibitor (**1**, 7.2 μM) decreases the extent of WT-TTR (3.6 μM) amyloid formation (pH 4.4) by 90% over a time course of 72 h. The X-ray cocrystal structure of TTR·$\mathbf{1}_2$ reveals that **1** exerts its impressive activity by binding exclusively to the outer portion of each thyroxine binding site.[33] This provides the opportunity to modify **1** with substructures that project into the inner cavity of the thyroxine binding pocket, which should increase their affinity and, most importantly, their selectivity for binding to TTR in human blood.

Herein, we utilize structure-based design principles to append aromatic substituents onto the dibenzofuran-4,6-dicarboxylic acid core structure at the C1 position using three different types of linkages, affording exceptional amyloidogenesis inhibitors. These display increased affinity and greatly increased binding selectivity to TTR over that of all the other plasma proteins, relative to lead compound **1**.[47] Moreover, we have demonstrated that these compounds function by imposing kinetic stabilization on the TTR tetramer. Hence, there is reason to be optimistic that they will be clinically useful, based on the analogy with interallelic trans suppression, provided they exhibit suitable pharmacology and toxicology profiles, the analysis of which is beyond the scope of this contribution.[31,35,43]

Design and Synthesis

Figure 1A depicts the two symmetry-equivalent binding modes of **1** (green and yellow) within one of the TTR thyroxine

(15) Hornsten, R.; Wiklund, U.; Olofsson, B.-O.; Jensen, S. M.; Suhr, O. B. *Transplantation* **2004**, *78*, 112−116.
(16) Dubrey, S. W.; Davidoff, R.; Skinner, M.; Bergethon, P.; Lewis, D.; Falk, R. H. *Transplantation* **1997**, *64*, 74−80.
(17) Pfeffer, B. A.; Bacerra, S. P.; Borst, D. E.; Wong, P. *Mol. Vision* **2004**, *10*, 23−30.
(18) Hornberg, A.; Eneqvist, T.; Olofsson, A.; Lundgren, E.; Sauer-Eriksson, A. E. *J. Mol. Biol.* **2000**, *302*, 649−669.
(19) Blake, C. C. F.; Geisow, M. J.; Oatley, S. J.; Rerat, B.; Rerat, C. *J. Mol. Biol.* **1978**, *121*, 339−356.
(20) Monaco, H. L.; Rizzi, M.; Coda, A. *Science* **1995**, *268*, 1039−1041.
(21) Nilsson, S. F.; Rask, L.; Peterson, P. A. *J. Biol. Chem.* **1975**, *250*, 8554−8563.
(22) Colon, W.; Kelly, J. W. *Biochemistry* **1992**, *31*, 8654−8660.
(23) Kelly, J. W. *Curr. Opin. Struct. Biol.* **1996**, *6*, 11−17.
(24) Lai, Z.; Colon, W.; Kelly, J. W. *Biochemistry* **1996**, *35*, 6470−6482.
(25) Lashuel, H. A.; Wurth, C.; Woo, L.; Kelly, J. W. *Biochemistry* **1999**, *38*, 13560−13573.
(26) Liu, K.; Cho, H. S.; Lashuel, H. A.; Kelly, J. W.; Wemmer, D. E. *Nat. Struct. Biol.* **2000**, *7*, 754−757.
(27) McCutchen, S. L.; Lai, Z.; Miroy, G. J.; Kelly, J. W.; Colon, W. *Biochemistry* **1995**, *34*, 13527−13536.
(28) Reixach, N.; Deechongkit, S.; Jiang, X.; Kelly, J. W.; Buxbaum, J. N. *Proc. Natl. Acad. Sci. U.S.A.* **2004**, *101*, 2817−2822.
(29) Sousa, M. M.; Cardoso, I.; Fernandes, R.; Guimaraes, A.; Saraiva, M. J. *Am. J. Pathol.* **2001**, *159*, 1993−2000.
(30) Coelho, T.; Carvalho, M.; Saraiva, M. J.; Alves, I. L.; Almeida, M. R.; Costa, P. P. *J. Rheumatol.* **1993**, *20*, 179−179.
(31) Hammarstrom, P.; Wiseman, R. L.; Powers, E. T.; Kelly, J. W. *Science* **2003**, *299*, 713−716.
(32) Hammarstrom, P.; Schneider, F.; Kelly, J. W. *Science* **2001**, *293*, 2459−2462.
(33) Klabunde, T.; Petrassi, H. M.; Oza, V. B.; Raman, P.; Kelly, J. W.; Sacchettini, J. C. *Nat. Struct. Biol.* **2000**, *7*, 312−321.
(34) Razavi, H.; Palaninathan, S. K.; Powers, E. T.; Wiseman, R. L.; Purkey, H. E.; Mohamedmohaideen, N. N.; Deechonkit, S.; Chiang, K. P.; Dendle, M. T. A.; Sacchettini, J. C.; Kelly, J. W. *Angew. Chem.* **2003**, *42*, 2758−2761.
(35) Cohen, F. E.; Kelly, J. W. *Nature* **2003**, *426*, 905−909.
(36) Miroy, G. J.; Lai, Z.; Lashuel, H. A.; Peterson, S. A.; Strang, C.; Kelly, J. W. *Proc. Natl. Acad. Sci. U.S.A.* **1996**, *93*, 15051−15056.
(37) Peterson, S. A.; Klabunde, T.; Lashuel, H.; Purkey, H.; Sacchettini, J. C.; Kelly, J. W. *Proc. Natl. Acad. Sci. U.S.A.* **1998**, *95*, 12956−12960.
(38) Baures, P. W.; Peterson, S. A.; Kelly, J. W. *Bioorg. Med. Chem.* **1998**, *6*, 1389−1401.
(39) Baures, P. W.; Oza, V. B.; Peterson, S. A.; Kelly, J. W. *Bioorg. Med. Chem.* **1999**, *7*, 1339−1347.
(40) Petrassi, H. M.; Klabunde, T.; Sacchettini, J.; Kelly, J. W. *J. Am. Chem. Soc.* **2000**, *122*, 2178−2192.
(41) McCammon, M. G.; Scott, D. J.; Keetch, C. A.; Greene, L. H.; Purkey, H. E.; Petrassi, H. M.; Kelly, J. W.; Robinson, C. V. *Structure* **2002**, *10*, 851−863.
(42) Oza, V. B.; Smith, C.; Raman, P.; Koepf, E. K.; Lashuel, H. A.; Petrassi, H. M.; Chiang, K. P.; Powers, E. T.; Sacchettini, J.; Kelly, J. W. S *J. Med. Chem.* **2002**, *45*, 321−332.
(43) Sacchettini, J. C.; Kelly, J. W. *Nat. Rev. Drug Discov.* **2002**, *1*, 267−275.
(44) Green, N. S.; Palaninathan, S. K.; Sacchettini, J. C.; Kelly, J. W. *J. Am. Chem. Soc.* **2003**, *125*, 13404−13414.
(45) Adamski-Werner, S. L.; Palaninathan, S. K.; Sacchettini, J. C.; Kelly, J. W. *J. Med. Chem.* **2004**, *47*, 355−374.
(46) Miller, S. R.; Sekijima, Y.; Kelly, J. W. *Lab. Invest.* **2004**, *84*, 545−552.
(47) Purkey, H. E.; Dorrell, M. I.; Kelly, J. W. *Proc. Natl. Acad. Sci. U.S.A.* **2001**, *98*, 5566−5571.

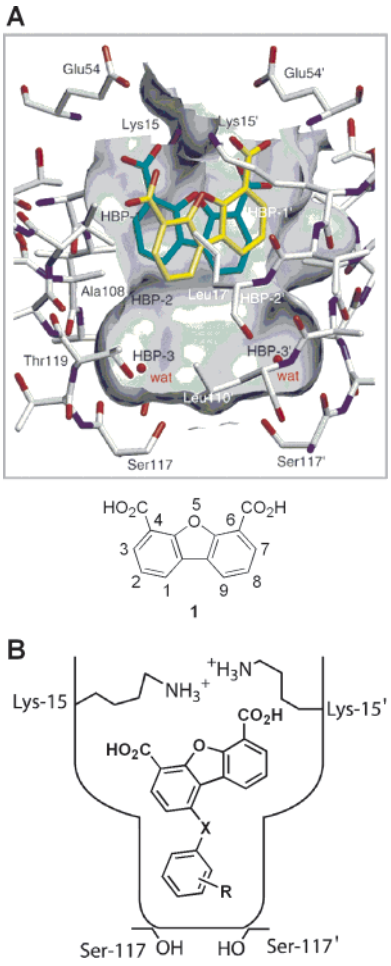

Figure 1. (A) X-ray crystallographic structure of TTR·$\mathbf{1}_2$ depicting one of the ligand binding sites (figure adapted from reference 33). The residues lining the binding site are displayed as stick models (oxygen in red, nitrogen in blue, and carbon in gray), with the protein's Connolly surface depicted in gray. Compound **1** is shown in both of its C_2 symmetry equivalent binding modes (yellow and green). The binding channel has three sets of depressions referred to as the halogen binding pockets (HBPs) because they interact with the iodines of thyroxine. Compound **1** occupies only the outer portion of the binding pocket and fills both HBP1 and 1′. The carboxylic acids of **1** are in proximity to the ϵ-NH_3^+ of K15 and K15′. (B) Line drawing representation of the design of the C1-substituted-dibenzofuran-4,6-dicarboxylic acids placed in the thyroxine binding pocket where X represents either an NH, O, or direct C_{aryl}−C_{aryl} linkage (not shown). R represents the substituents of the aryl ring envisioned to complement the inner binding cavity of TTR.

binding sites, the surface of which is outlined in gray.[33] The carboxylates at the 4 and 6 positions make electrostatic interactions with the ϵ-NH_3^+ groups of Lys 15 and 15′ at the entrance to the thyroxine binding site. Removal of one of the carboxylates renders dibenzofuran much less active, as does varying the carboxylate spacing from the aromatic ring in most cases (Figure S1). Inspection of the TTR·$\mathbf{1}_2$ crystal structure in **Figure 1A** reveals that the dibenzofuran ring nicely complements the shape and hydrophobicity of the outer portion of the thyroxine binding cavity and that there is a large amount of unoccupied volume in the inner portion of the thyroxine binding site with **1** bound. Based on this structure, it is clear that a substituent, such as an aryl ring, could be projected into the inner portion of the binding site by attaching it to the C1 position of the dibenzofuran ring of **1**. As shown in Figure 1B, such a substituent could be linked to a dibenzofuran scaffold through a heteroatom (N or O) or directly via a C_{aryl}−C_{aryl} bond (not shown). Aromatic substituents (Figure 2) were chosen to interact with either the halogen binding pockets or hydrogen bonding substructures within the inner cavity based on the envisioned orientation of the phenyl ring in the inner binding cavity and previous SAR data from other chemical series thought to position their aryl rings similarly.[31,33,34,36−46]

The synthesis of C1-substituted dibenzofuran-based inhibitors commenced with the radical phenolic homocoupling of commercially available 2,4-di-*tert*-butyl-6-bromophenol (**2**) to afford the dibenzofuran derivative **3** using potassium hexacyanoferrate (III) as previously reported (Scheme 1).[48] This tetra-*tert*-butyl dibenzofuran derivative was subjected to transalkylation in toluene to form 1-hydroxydibenzofuran (**4**) in 33% overall yield from **2** (alternative strategies for the synthesis of this intermediate have appeared).[49,50] After protection of the phenol, silyl ether **5** was selectively ortho metalated at the 4- and 6-positions with *sec*-butyllithium (the triisopropylsilyl group on the 1-oxygen precludes it from acting as a metalation director).[51] The dianion was quenched with gaseous CO_2 and esterified to afford **6**, which was then deprotected with TBAF and converted to triflate **8** in high overall yield.

Selected anilines were coupled to triflate **8** using a palladium-mediated *N*-arylation reaction developed by Buchwald and Hartwig to afford dibenzofuran-based biarylamine analogues **9**−**23** (Scheme 2).[52,53] To append an aryl ether to the C1-position of dibenzofuran, phenol **7** and several phenylboronic acids were cross-coupled using the copper-mediated biaryl ether coupling methodology of Chan and Evans, affording compounds **39**−**43**.[54,55] Compound **8** was also subjected to Suzuki coupling conditions in the presence of several phenylboronic acids to afford the dibenzofuran-based biaryl analogues **49**−**59**.[56] Saponification of the methyl esters in these precursors afforded the desired dibenzofuran-4,6-dicarboxylic acid amines (**24**−**38**), ethers (**44**−**48**), and biaryls (**60**−**70**) to be evaluated as potential TTR amyloidogenesis inhibitors.

Results

Two of the most important characteristics of an effective small molecule amyloidogenesis inhibitor are the ability to bind with high affinity and selectively to TTR in blood and to stabilize the native tetrameric structure of TTR.[31,34,47] Inhibition efficacy (compounds **24**−**38**, **44**−**48**, and **60**−**70**) was first evaluated using recombinant TTR in a partially denaturing buffer that promotes amyloidogenesis (pH 4.4, 37 °C). As a follow up, the ability of effective inhibitors to bind to TTR selectively over all the other proteins in human plasma was assessed.

Evaluating the Dibenzofuran-Based Compounds As Amyloidogenesis Inhibitors. TTR amyloid inhibition efficacy was probed using a stagnant fibril formation assay described

(48) Tashiro, M.; Yoshiya, H.; Fukata, G. *Synthesis* **1980**, *6*, 495−496.
(49) Labiad, B.; Villemin, D. *Synthesis* **1989**, 143−144.
(50) Lee, Y. R.; Suk, J. Y.; Kim, B. S. *Org. Lett.* **2000**, *2*, 1387−1389.
(51) Snieckus, V. *Chem. Rev.* **1990**, *90*, 879−933.
(52) Louie, J. D.; Michael S.; Hamann, B. C.; Hartwig, J. F. *J. Org. Chem.* **1997**, *62*, 1268−1273.
(53) Wolfe, J. P. B. *Tetrahedron Lett.* **1997**, *38*, 6359−6362.
(54) Chan, D. M. T.; Monaco, K. L.; Wang, R.-P.; Winters, M. P. *Tetrahedron Lett.* **1998**, *39*, 2933−2936.
(55) Evans, D. A.; Katz, J. L.; West, T. R. *Tetrahedron Lett.* **1998**, *39*, 2937−2940.
(56) Suzuki, A. *Mod. Arene Chem.* **2002**, 53−106.

A

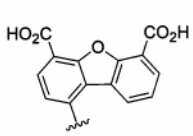

Inhibitor	Aryl subs. (R)	% Fibril formation	Plasma binding stoichiometry
1		53	0
24	H	35	1.22
25	2-CF_3	25	1.69
26	3-CF_3	32	1.31
27	3-Cl	36	1.25
28	3-Br	41	1.10
29	3,5-F_2	48	1.34
30	3,5-Cl_2	30	1.19
31	3,5-$(CF_3)_2$	35	0
32	2,4-Cl_2	41	0.72
33	3-CO_2H	24	0.61
34	3,5-CO_2H	76	ND
35	4-CO_2H	38	0
36	2-F	16	1.23
37	2-Cl-5-F	26	1.10
38	2-Cl	32	1.27
44	H	38	1.01
45	3-CF_3	38	1.24
46	3,5-F_2	34	1.19
47	3,5-Cl_2	36	1.98
48	3,5-Br_2	35	1.68
60	H	23	1.29
61	3-CF_3	27	0.87
62	3,5-F_2	24	1.16
63	3,5-Cl_2	19	1.16
64	3,5-$(CF_3)_2$	30	1.54
65	3-F	30	1.20
66	3-Cl	33	1.25
67	2-F	15	0.65
68	2-Cl	38	0.86
69	3-CO_2H	24	0.68
70	4-CO_2H	43	0.71

B

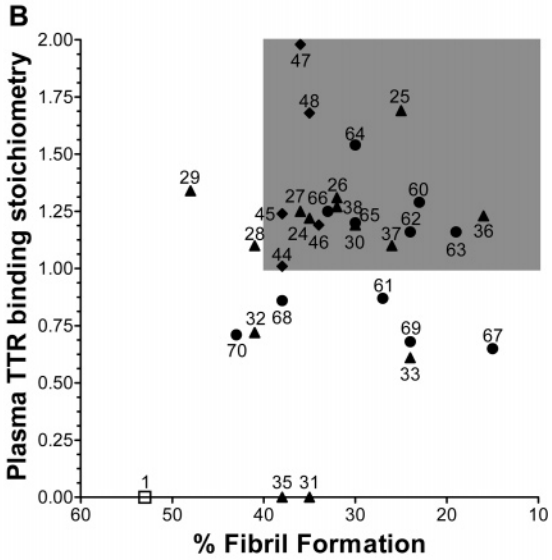

Figure 2. (A) Summary of dibenzofuran-based amyloid inhibition activity (3.6 μM) against WT-TTR (3.6 μM) fibril formation (pH 4.4, 72 h, 37 °C) in vitro and binding stoichiometry of these inhibitors to TTR in human blood plasma. % Fibril formation (*f.f.*) values in the middle column represent the extent of *f.f.*, and thus inhibitor efficacy, relative to WT-TTR *f.f.* in the absence of inhibitor (assigned to be 100%). Complete inhibition is equivalent to 0% *f.f.* Measurement error is ±5%. The right column depicts the observed stoichiometry of inhibitor (dosed at 10.8 μM, ~2−3× the concentration of plasma TTR) bound to TTR in blood plasma as determined using the antibody capture method as described herein and elsewhere.[47] Measurement error is ±0.15. (B) Inhibitor binding stoichiometry to TTR in plasma plotted vs fibril formation inhibition efficacy in vitro (omitting data for inhibitor **34**, which was not analyzed for binding selectivity due to poor *f.f.* inhibition). The area shaded gray corresponds to our definition of high activity and high selectivity (<40% fibril formation and a binding stoichiometry >1). Biaryls are identified as ●, biarylamines as ▲, and biaryl ethers as ◆; the lead compound **1** = □.

previously, wherein partial denaturation was triggered by acidification (pH 4.4, 37 °C).[22] Briefly, a test compound (7.2 or 3.6 μM) is incubated with TTR (3.6 μM) for 30 min in pH 7 buffer. Amyloidogenesis is then initiated by lowering the pH to 4.4, where maximal fibril formation is observed with WT-TTR after 72 h (37 °C). The turbidity in the presence of a potential inhibitor (T_{test}) is compared to that of a solution lacking a test compound ($T_{control}$). Exceptional inhibitors yield 0% fibril formation, whereas compounds not functioning as an inhibitor afford 100% fibril formation. From experience we know that excellent inhibitors allow <10% fibril formation at a small molecule concentration of 7.2 μM and <40% fibril formation at a concentration equal to that of WT-TTR (3.6 μM).[31,33,34,36−46] Of the 31 compounds evaluated, all but one (**34**) completely inhibit fibril formation at a concentration twice that of TTR (7.2 μM inhibitor), Figure S2 (at 7.2 μM there is enough test compound added to occupy both of the binding sites of TTR ($TTR{\cdot}I_2$), provided their dissociation constants are both in the low nanomolar range at pH 4.4). Small molecules typically bind to TTR with negative cooperativity; hence, K_{d1} and K_{d2} are often separated by 1 or 2 orders of magnitude. Therefore, when both the ligand and TTR are at equal concentrations, a population

Scheme 1. Synthesis of 1-Hydroxydibenzofuran-4,6-dicarboxylate Dimethyl Ester and the Corresponding Triflate[a]

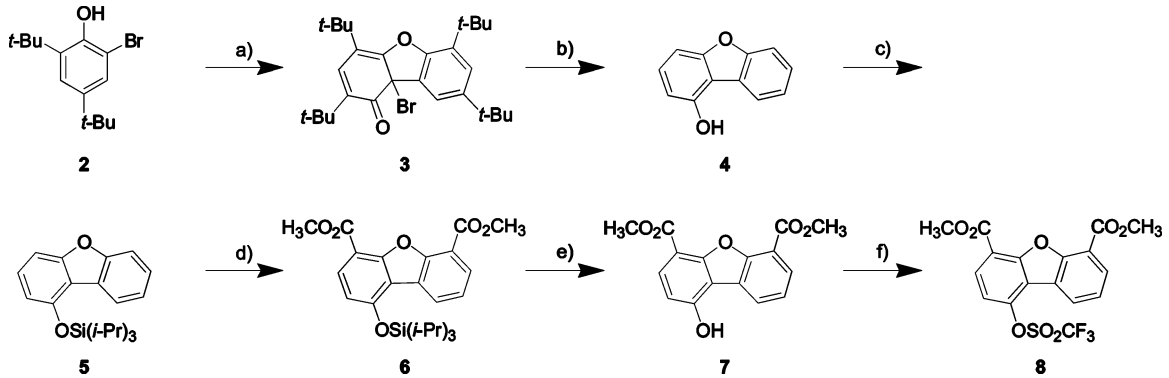

[a] Conditions: a) $K_3[Fe(CN)_6]$, KOH, H_2O, benzene; b) $AlCl_3$, toluene, 33% for both steps; c) TIPSCl, DMAP, CH_2Cl_2, 77%; d) *sec*-BuLi, Et_2O, −78 °C, gaseous CO_2, $TMSCHN_2$, 43%; e) TBAF, THF, 97%; f) Tf_2O, pyridine, 92%.

Scheme 2. Synthesis of 1-Phenyl-, Phenoxy-, and Phenylamine-dibenzofuran-4,6-dicarboxylate Dimethyl Esters and the Corresponding Dicarboxylates[a]

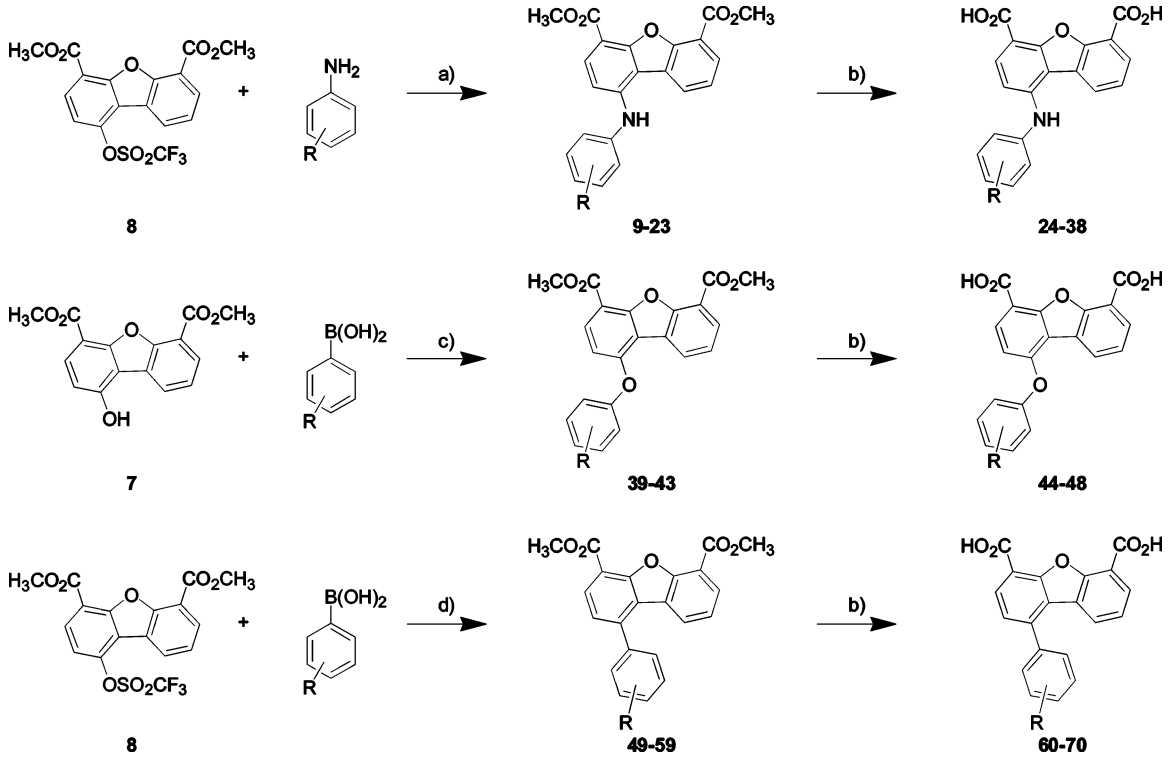

[a] Conditions: a) $Pd_2(DBA)_3$, (±)binap, Cs_2CO_3, toluene 100 °C; b) LiOH·H_2O, THF/MeOH/H_2O (3:1:1); c) $Cu^{II}(OAc)_2$, pyridine, 4 Å molecular sieves, CH_2Cl_2; d) $Pd(PPh_3)_4$, LiCl, aq. Na_2CO_3, toluene, MeOH, 80°C.

of TTR·I, TTR·I_2, and unliganded TTR is observed, dictated by the dissociation constants. It is now established by other studies that inhibitor occupancy of only one of the two TTR binding sites is sufficient to stabilize the entire tetramer against amyloidogenesis.[57] This is further supported by the observation herein that 26 of these dibenzofurans are excellent TTR amyloidogenesis inhibitors (<40% fibril formation) at a concentration equal to that of TTR (3.6 μM, Figure 2A). Representative small molecules from all three series (**25**, **26**, **27**, **30**, **45**, **47**, **62**; 3.6 μM) were subjected to the acid-mediated amyloidogenic conditions (pH 4.4, 37 °C, 72 h) in the absence of TTR, revealing no measurable precipitation.

Evaluating the Plasma TTR Binding Selectivity of the Dibenzofuran-Based Inhibitors. Inhibitor binding selectivity to TTR in human blood plasma was assessed using a previously established antibody capture method.[47] In this evaluation, inhibitors (10.8 μM, ~2−3× the natural concentration of TTR) are incubated with human blood plasma for 24 h at 37 °C. Quenched sepharose resin is then added to the plasma to remove any small molecules that would bind to the resin as opposed to TTR. TTR and any TTR-bound small molecule is then immunocaptured using a polyclonal TTR antibody covalently attached to sepharose resin. After washing the resin (5 × 10-min washes), the antibody−TTR complex is dissociated at high pH and analyzed by RP-HPLC. The relative stoichiometry between TTR and inhibitor is then calculated from their HPLC peak areas using standard curves. Wash-associated losses are typically observed for inhibitors that have high dissociation rates; therefore, this analysis can underestimate true binding stoichiometry but gives faithful results for compounds exhibiting low

(57) Wiseman, R. L.; Johnson, S. M.; Kelker, M. S.; Foss, T.; Wilson, I. A.; Kelly, J. W. *J. Am. Chem. Soc.* **2005**, *127*, 5540−5551.

dissociation constants and off-rates. Twenty-one inhibitors exhibit a binding stoichiometry exceeding one (Figure 2A; two being the maximal binding stoichiometry possible), 19 of which exhibit <40% fibril formation at a concentration of 3.6 μM (Figure 2B, shaded box). The high plasma TTR binding selectivities observed are remarkable, considering that the parent dibenzofuran-4,6-dicarboxylic acid (**1**) displays no binding selectivity to TTR, demonstrating the importance of the C1 aryl substituent in terms of endowing binding selectivity to TTR over all the other plasma proteins.

Stabilization of the Tetrameric Quaternary Structure under Amyloidogenic Conditions. To ensure that these C1-arylated dibenzofurans inhibit TTR fibril formation by native state stabilization (i.e., tetramer stabilization), we studied the TTR quaternary structure by analytical ultracentrifugation after a preincubation period of 72 h under amyloidogenic conditions (pH 4.4, 37 °C). In the presence of **27** (7.2 μM), TTR (3.6 μM) was found to have hydrodynamic molecular weights of 57.1 ± 0.3 and 55.1 ± 0.4 kDa by sedimentation velocity (Figure 3A) and equilibrium analytical ultracentrifugation (Figure 3B), respectively, comparable to the expected molecular weight of tetrameric TTR (55.0 kDa). In the absence of **27**, TTR aggregated into very high molecular weight oligomers that sedimented rapidly in the ultracentrifugation experiment (data not shown).

Do the Dibenzofuran-Based Inhibitors Impose Kinetic Stabilization on TTR? The ability of these inhibitors to impose kinetic stability on tetrameric TTR is best evaluated by assessing the rate of TTR tetramer dissociation.[31,58] Under acidic conditions (pH 4.4, 37 °C) tetramer dissociation leads to amyloidogenesis, whereas in the presence of chaotropes (6 M urea, 25 °C) tetramer dissociation leads to monomer unfolding. The influence of inhibitors **25**, **47**, and **64**, representing the three structural classes of dibenzofuran-based inhibitors, on the rates of tetramer dissociation under acid- and urea-mediated denaturing conditions was probed. TTR amyloidogenesis mediated by partial acidification is dramatically slowed in a dose-dependent fashion relative to control (no inhibitor) by **25**, **47**, and **64** (Figure 4A). The rate of TTR tetramer dissociation in 6 M urea is easily monitored by linking the slow quaternary structural changes to rapid tertiary structural changes that are easily monitored by spectroscopic methods.[58] The rate of TTR tetramer (3.6 μM) dissociation monitored by far-UV circular dichroism (CD) is markedly slowed in a dose-dependent fashion in 6 M urea by **25**, **47**, and **64** (Figure 4B). These results are consistent with differential stabilization of the ground state vs the dissociative transition state by the binding of **25**, **47**, and **64**.

Discussion

All but one of the C1-aryl substituted dibenzofurans (7.2 μM) are exceptional inhibitors of WT-TTR (3.6 μM) acid-mediated fibril formation in vitro (pH 4.4, 37 °C), even those bearing unsubstituted aryl rings (Figure S2). The only dibenzofuran-based inhibitor that was not as effective against TTR amyloidogenesis was **34**, bearing potentially four negative charges. Because all the compounds completely inhibited TTR fibril formation (within the ±5% experimental error), no structure−activity relationships (SAR) are deducible from the 7.2 μM inhibitor data. However, parts A and B of Figure 2 reveal a range of inhibitor efficacy at an inhibitor concentration equal to that of TTR (3.6 μM), allowing some SAR conclusions to be drawn, limited by the 31 analogues prepared and the experimental error. Notably, all the inhibitors (except **34**) display increased potency relative to that of the parent compound (**1**) at 3.6 μM (Figure 2B). Most importantly, of the 30 inhibitors exhibiting increased potency, all but two (**31** and **35**) exhibit dramatically increased binding selectivity to TTR in human blood plasma. The exceptional binding selectivity exhibited by the C1-substituted inhibitors is ideal for inhibiting TTR amyloidogenesis in complex biological systems.

Comparison of the four C1-aryl substitution patterns (H, 3-CF_3, 3,5-F_2, and 3,5-Cl_2) found in all three inhibitor series reveals that the inhibitors having their aryl rings directly linked

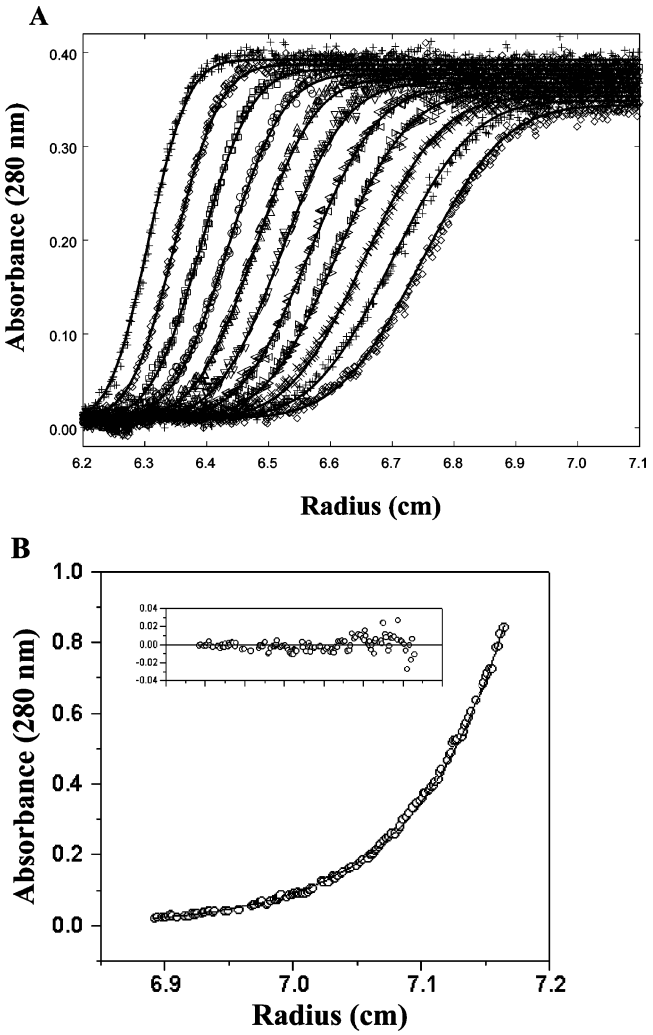

Figure 3. Sedimentation velocity (A) and equilibrium ultracentrifugation studies (B) on TTR (3.6 μM) after being preincubated with **27** (7.2 μM, 30 min, pH 7) and after another incubation period where the pH was dropped to 4.4 for 72 h at 37 °C, a time frame that results in near maximal amyloid formation in the absence of inhibitor. (A) Velocity analysis: overlay of data sets taken 15 min apart at 50,000 rpm. The data (symbols) fit to a single ideal species model (solid line) with a MW of 57.1 ± 0.3 kDa. (B) TTR equilibrium concentration gradient observed after a 24 h application of centrifugal force to the sample employing at a speed of 17,000 rpm. The data (○) fit to a single ideal species model (solid line) with a MW of 55.1 ± 0.4 kDa. The residuals, the difference between experimental and fitted data, are shown in the inset.

(58) Hammarstrom, P.; Jiang, X.; Hurshman, A. R.; Powers, E. T.; Kelly, J. W. *Proc. Natl. Acad. Sci. U.S.A.* **2002**, *99*, 16427−16432.

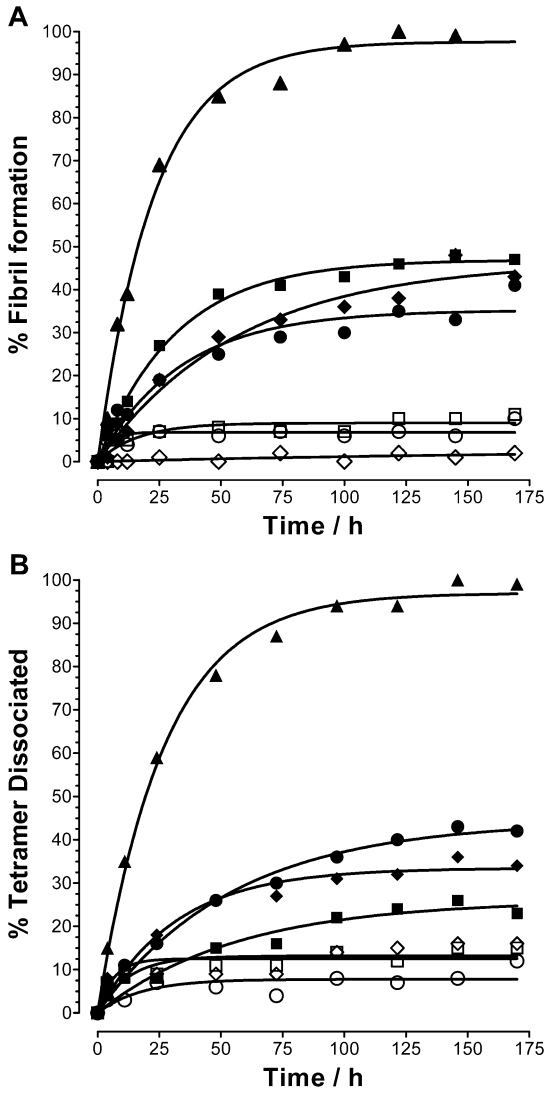

Figure 4. (A) Timecourse analysis of WT-TTR (3.6 μM) fibril formation mediated by partial acid denaturation (pH 4.4, 37 °C) in the absence (▲) and presence of inhibitors **25** (7.2 μM = ○; 3.6 μM = ●), **47** (7.2 μM = □; 3.6 μM = ■), and **64** (7.2 μM = ◇; 3.6 μM = ◆), as measured by turbidity at 500 nm. (B) Timecourse analysis of WT-TTR (3.6 μM) tetramer dissociation (6.0 M urea, 25 °C) in the absence (▲) and presence of inhibitors **25**, **47**, and **64** at 7.2 and 3.6 μM as defined in graph A. Slow tetramer dissociation is not detectable by far-UV CD spectroscopy, but this process is linked to rapid (~500,000× faster) monomer denaturation as monitored by loss of β-sheet content, easily followed by CD spectroscopy.

to C1 of the dibenzofuran skeleton, hereafter referred to as the biaryls, display slightly increased inhibitor potency relative to that of their biarylamine and biaryl ether counterparts (Figure 2A). This may be due to structural differences that enable the rings to be oriented differently within the inner binding cavity; however, we caution that this preference may not hold in a very large analogue series. It could be argued with the same qualifiers that the other two series produce the most selective TTR binders in plasma; however, the SAR here is confounded by the fact that as many as 100 proteins are competing for these inhibitors. While it is not surprising that the most potent inhibitors have 2-F or 3,5-Cl_2 substituents (**36**, **63**, and **67**), likely picking up the halogen binding pockets in the thyroxine binding site, it is somewhat surprising that the 3-CO_2H-substituted aryl inhibitors **33** and **69** are among the most potent (although their plasma binding selectivity to TTR is modest). Previous crystallographic results on simple biphenyl and biphenylamine inhibitors demonstrate that it can be preferable to have the carboxyl-bearing aryl ring in the inner binding cavity (enabling H-bonding to S117 and T119).[33,42,45]

Appending aryl groups to the C1 position not only increases inhibitor potency, but more importantly dramatically increases plasma binding selectivity to TTR, presumably by increasing binding affinity for TTR over the other plasma proteins. The superior binding selectivity of the C1-aryl-substituted dibenzofuran-based inhibitors to TTR in plasma is clearly demonstrated by the fact that about two-thirds of the compounds prepared display a TTR binding stoichiometry >1. This is exceedingly interesting as the screening hit **1**, utilizing only the outer cavity of TTR for binding, displays no measurable binding selectivity to TTR in plasma. Previous experience with amyloidogenesis inhibitors of diverse chemical structure reveals that very few members display binding stoichiometries exceeding 1.[31,33,34,36−46] The area of Figure 2B shaded in gray contains dibenzofuran-based compounds that meet the criteria for high in vitro activity (<40% fibril formation) and high binding selectivity (>1 equiv bound to TTR in plasma). The most important point is that the activity and binding selectivity of almost all of the dibenzofuran-based inhibitors, especially those in the gray box (Figure 2B), are sufficient to kinetically stabilize TTR in plasma should they display desirable oral bioavailability, pharmacokinetic, and toxicity profiles.

It is not surprising that inhibitor efficacy in vitro (3.6 μM) and inhibitor binding selectivity (10.8 μM) to TTR in plasma do not correlate (Figure 2B). Compounds that exhibit superior binding selectivity to TTR over that of all of the other plasma proteins should be excellent inhibitors of fibril formation. However, the converse is not necessarily true: excellent inhibitors need not display high TTR plasma binding selectivity. Excellent inhibitors that display high TTR plasma binding selectivity are the most useful compounds in humans because these can selectively stabilize the TTR native state over the dissociative transition state and impart kinetic stabilization on TTR in a protein-rich biological fluid. Inhibitor binding constants to TTR are important because the extent of kinetic stabilization is proportional to the binding constants. However, focusing on binding constants and potency in vitro can be misleading because compounds can be excellent TTR amyloidogenesis inhibitors in vitro, but bind to other plasma proteins and therefore be rendered useless in humans.[47] Potent in vitro inhibitors not displaying good binding selectivity to TTR likely interact with other plasma proteins, such as albumin.[47] Because the dibenzofuran inhibitors display unprecedented binding selectivity and inhibitor potency as a group relative to inhibitors characterized heretofore,[31,33,34,36−46] these are ideal for further pharmacological evaluation. Because TTR is the tertiary carrier of T_4, more than 99% of its binding sites are unoccupied; therefore, inhibitor binding to TTR should not perturb T_4 homeostasis.

In summary, the C1-substituted dibenzofuran-based TTR amyloidogenesis inhibitors are promising because of their amyloid inhibition potency in vitro, their superb binding selectivity to TTR in plasma, their slow TTR dissociation rates (which must be the case to see high plasma selectivity by the method utilized herein), their ability to impose kinetic stabilization upon the TTR tetramer, their chemical stability in plasma, and their chemical stability at low pH (making them excellent

candidates for oral administration). There is reason to be optimistic that these inhibitors have the potential to be generally useful for the treatment of TTR amyloid diseases, including SSA, FAP, and FAC, because kinetic stabilization of TTR is known to ameliorate FAP.[30,31,32]

Experimental Section

The procedures used for bacterial expression of TTR,[24] the stagnant fibril formation assay,[22,24] the blood plasma binding selectivity assay,[47] and analytical ultracentrifugation[59] have all been described in detail previously.

Time Course Analysis of WT-TTR Fibril Formation Inhibition by Compounds 25, 47, and 64. Compounds **25**, **47**, and **64** were dissolved in DMSO to provide 7.2 mM primary stock solutions (10× stocks), from which 5- and 10-fold DMSO dilutions yielded 1.44 mM (2×) and 0.72 mM (1×) secondary stock solutions, respectively. To disposable cuvettes were added 495 μL of 0.4 mg/mL (7.2 μM) WT-TTR solution (10 mM sodium phosphate, 100 mM KCl, and 1 mM EDTA, pH 7.2) and 5 μL of either the 1.44 or 0.72 mM inhibitor secondary stock solutions; these were vortexed briefly and then incubated for 30 min at 25 °C. The pH was then adjusted to 4.4 with addition of 500 μL of acidic buffer (100 mM acetate, 100 mM KCl, 1 mM EDTA, pH 4.2), and the final 1 mL solutions were vortexed again and incubated in the dark at 37 °C without agitation. At 0, 4, 8, 12, 25, 49, 74, 100, 122, 145, and 169 h time points after acidification, the solutions were vortexed, and the turbidity at 500 nm was measured. Control samples containing 5 μL of pure DMSO were prepared and analyzed as above for comparison. Small molecule and TTR control samples were prepared in groups of 10 to prevent disturbance of the cuvettes during incubation. Samples were discarded after their turbidities were measured.

Time Course Analysis of WT-TTR Tetramer Dissociation Inhibition by Compounds 25, 47, and 64 Evaluated by Linked-Monomer Unfolding in Urea. Compounds **25**, **47**, and **64** were dissolved in DMSO to provide 10 mM primary stock solutions, from which 10-fold EtOH dilutions yielded 1 mM secondary stock solutions. To 2-mL Eppendorf tubes were added 200 μL of 1.0 mg/mL (18 μM) WT-TTR solution (50 mM sodium phosphate, 100 mM KCl, and 1 mM EDTA, pH 7.2) and either 7.2 or 3.6 μL (2× and 1×, respectively) of 1 mM inhibitor secondary stock solutions; these were vortexed briefly and incubated for 15 min at 25 °C. The TTR·inhibitor solutions (100 μL) were added to 900 μL of urea buffer (6.67 M urea, 50 mM sodium phosphate, 100 mM KCl, 1 mM EDTA, pH 7.2), and the final 1 mL solutions were vortexed again and incubated in the dark at 25 °C without agitation. At 0, 4, 11, 24, 49, 73, 97, 122, 146, and 170 h time points after mixing with urea, the CD spectra were measured between 218 and 215 nm, with scanning every 0.5 nm and averaging for 5 s. After measurements were taken, samples were returned to their respective Eppendorf tubes and incubation was continued. Control samples containing 7.2 μL of 10% DMSO in EtOH were prepared and analyzed as above for comparison. The CD amplitude values were averaged between 215 and 218 nm to determine the extent of β-sheet loss throughout the experiment. TTR tetramer dissociation is linked to the rapid (~500,000× faster) monomer denaturation as measured through this β-sheet loss.[58]

Inhibitor Synthesis. Reagents for chemical synthesis were purchased from commercial suppliers and used without further purification unless otherwise stated. Thin-layer chromatography on silica gel 60 F_{254} coated aluminum plates (EM Sciences) or analytical reverse-phase high performance liquid chromatography (HPLC) was used to monitor reaction progress. HPLC was performed using a Waters 600E multi-solvent delivery system employing a Waters 486 tunable absorbance detector and a Waters 717 plus auto sampler. A C18 Western Analytical column was used (model 033-715, 150 Å pore size, 3 μm particles) for all reverse-phase HPLC analyses. An acetonitrile/water/trifluoroacetic acid solvent system was used; solvent A in the proportions of 4.8%, 95%, and 0.2%, respectively, while solvent B was of 95%, 4.8%, and 0.2%, respectively. Following 2 min of isocratic flow at 100% A, a linear gradient of 0 to 100% B over 8 min was run at 1.5 mL/min. All flash chromatography was accomplished using 230−400 mesh silica gel 60 (EM Sciences). ^{1}H- and ^{13}C NMR spectra were recorded at 300, 400, 500, or 600 MHz on Bruker spectrometers. Chemical shifts are reported in parts per million downfield from the internal standard (Me_4-Si, 0.0 ppm).

(Dibenzofuran-1-yloxy)triisopropylsilane (5). To a dry 250-mL round-bottom flask was added phenol **4**[48] (492 mg, 2.67 mmol) and a stir bar, and the flask was capped with a septum. CH_2Cl_2 (5 mL) was added followed by DMAP (391 mg, 3.2 mmol) and triisopropylsilyl chloride (800 μL, 3.73 mmol). The resulting colorless solution became a white suspension overnight. The reaction was transferred to a 250-mL separatory funnel and washed with H_2O (3 × 10 mL). The aqueous layers were combined and extracted with CH_2Cl_2 (3 × 30 mL). The organic layers were combined, dried with $MgSO_4$, and concentrated under reduced pressure to afford a pale-yellow oil. The oil was purified by flash chromatography over silica (100% hexanes) to afford 0.70 g (77%) of **5** as a colorless oil. ^{1}H NMR (600 MHz, $CDCl_3$) δ 1.22 (d, J = 7.6 Hz, 18 H), 1.48 (s, J = 7.6 Hz, 3 H), 7.69 (t, J = 8.6 Hz, 1 H), 7.19 (d, J = 8.2 Hz, 1H), 7.27−7.33 (m, 1H), 7.36 (t, J = 7.5 Hz, 1 H), 7.44 (t, J = 8.2 Hz, 1 H), 7.56 (t, J = 8.2 Hz, 1 H), 8.16−8.20 (s, 1H); ^{13}C NMR (150 MHz, $CDCl_3$) δ 13.33, 18.04, 104.31, 111.02, 111.77, 115.74, 122.59, 122.61, 123.76, 126.09, 127.47, 152.18, 155.44, 157.67; MALDI-FTMS 341.1932 m/z $(M + H)^+$, $C_{21}H_{29}O_2Si$ requires 341.1931.

1-Triisopropylsilanyloxydibenzofuran-4,6-dicarboxylic Acid Dimethyl Ester (6). Silyl ether **5** (654 mg, 1.92 mmol) was added to a dry 50-mL round-bottom flask followed by Et_2O (7.4 mL) and TMEDA (0.87 mL, 5.77 mmol). The flask was cooled to −78 °C in an acetone/CO_2(s) bath for 10 min before adding *sec*-butyllithium (4.44 mL of a 1.3 M solution in cyclohexane, 5.77 mmol) over 10 min. The resulting orange suspension was allowed to warm to room temperature and stirred for 24 h. The flask was cooled again to −78 °C as described above, and a 15 psi stream of CO_2(g) was bubbled through the reaction suspension (the CO_2 was dried by passing it through a drying tube containing activated silica). Following initial addition of CO_2(g), the cooling bath was removed, and the reaction was stirred for 30 min. The reaction mixture was poured into a 1-L beaker containing ice/H_2O (50 mL). The solution was brought to pH 9 by the slow addition of 0.05 M KOH and then cooled to 0 °C with an ice/H_2O bath. The solution was acidified to pH 2 with 0.5 M HCl causing a white solid to precipitate. The aqueous suspension (pH 2) was transferred into a 1-L separatory funnel and extracted with EtOAc (5 × 50 mL). The combined extracts were dried with $MgSO_4$ and concentrated under reduced pressure to afford the crude diacid as an oil. The 100-mL flask containing the crude diacid was equipped with a stir bar, capped with a septum, and evacuated. The flask was then back-filled with argon. Anhydrous MeOH (2 mL) and ACS reagent grade benzene (8 mL) were added via syringe. Trimethylsilyldiazomethane ($TMSCHN_2$; 2.5 mL of a 2 M solution in hexanes, 5 mmol) was added slowly via syringe through the septum. Upon completion of the $TMSCHN_2$ addition the reaction was stirred for 10 min and the solvent removed under reduced pressure to afford a red oil. The residue was purified by flash chromatography over silica (15% EtOAc in hexanes) to afford 0.36 g (43%) of **6** as a white solid. ^{1}H NMR (600 MHz, $CDCl_3$) δ 1.18 (d, J = 7.6 Hz, 18 H), 1.47 (s, J = 7.6 Hz, 3 H), 4.07 (s, 3H), 4.10 (s, 3H), 7.64 (t, J = 8.6 Hz, 1 H), 7.44 (d, J = 7.8 Hz, 1H), 8.06 (d, J = 8.6 Hz, 1H), 8.12 (d, J = 1.4 Hz, 1H), 8.14 (d, J = 1.4 Hz, 1H); ^{13}C NMR (150 MHz, $CDCl_3$) δ 13.26, 17.87, 52.12, 52.38, 108.60, 112.40, 115.07, 115.60, 123.03, 124.48, 127.04, 128.91, 131.56, 147.92, 154.26, 156.47, 156.87, 165.06, 165.27; MALDI-FTMS 479.1874 m/z $(M + Na)^+$, $C_{25}H_{32}O_6SiNa$ requires 479.1860.

(59) Lashuel, H. A.; Lai, Z.; Kelly, J. W. *Biochemistry* **1998**, *37*, 17851−17864.

1-Hydroxydibenzofuran-4, 6-dicarboxylic Acid Dimethyl Ester (7). A dry 100-mL round-bottom flask was equipped with a stir bar, charged with **6** (363 mg, 0.95 mmol), capped with a septum, evacuated, and back-filled with argon. Anhydrous THF (6.3 mL) and tetrabutylammonium fluoride (1 M in THF, 1.2 mL, 1.19 mmol) were added to the reaction by syringe. The reaction was stirred for 1 h at room temperature and then poured into 30 mL of H_2O in a 250-mL separatory funnel. The aqueous layer was extracted with $CHCl_3$ (4 × 20 mL). The organic layers were combined, dried with $MgSO_4$, and concentrated under reduced pressure. The residue was purified by flash chromatography over silica (30% EtOAc in hexanes) to afford 0.23 g (97%) of **7** as a white solid. ^{1}H NMR (600 MHz, DMSO-d_6) δ 4.06 (s, 3H), 4.10 (s, 3H), 6.79 (d, J = 8.5 Hz, 1H), 7.43 (t, J = 7.7 Hz, 1H), 8.00 (d, J = 8.5 Hz, 1H); ^{13}C NMR (125 MHz, $CDCl_3$) δ 52.11, 52.48, 108.71, 112.61, 114.32, 115.55, 122.66, 125.48, 126.99, 129.55, 131.33, 147.77, 155.11, 156.45, 158.97, 165.01, 165.29; LC−MS m/z 301, $C_{16}H_{12}O_6$ requires 301.

1-Trifluoromethanesulfonyloxydibenzofuran-4,6-dicarboxylic Acid Dimethyl Ester (8). The triflation procedure previously described by Stille was used to synthesize **8**.[60] Phenol **7** (120 mg, 0.4 mmol) was added to a dry 10-mL round-bottom flask, which was then fitted with a septum. The solvent, anhydrous pyridine (2 mL), was added by syringe through the septum. The reaction mixture was cooled to 0 °C with an ice/H_2O bath. To initiate the reaction, trifluoromethanesulfonic anhydride (81 μL, 12 mmol) was added by syringe through the septum. The ice bath was removed, and the reaction was allowed to warm to room temperature and stirred overnight. The reaction mixture was poured into a 250-mL beaker containing 30 mL of an ice/H_2O slurry and transferred into a 125-mL separatory funnel. The aqueous layer was extracted with Et_2O (4 × 40 mL). The organic layers were combined, washed with saturated $CuSO_4$ (4 × 20 mL) and brine (2 × 20 mL), dried over $MgSO_4$; the Et_2O was then removed under reduced pressure to afford a slightly yellow solid. The solid was purified by flash chromatography over silica (30% EtOAc in hexanes) to afford 159 mg (92%) of **8** as a white solid. ^{1}H NMR (600 MHz, $CDCl_3$) δ 4.11 (s, 3H), 4.12 (s, 3H), 7.44 (d, J = 8.7 Hz, 1H), 7.56 (t, J = 7.8 Hz, 1H), 8.24 (d, J = 8.7 Hz, 1H), 8.26 (d, J = 7.8 Hz, 1H), 8.36 (d, J = 7.8 Hz, 1H); ^{13}C NMR (150 MHz, $CDCl_3$) δ 115.70, 116.19, 116.41, 122.09, 124.51, 127.63, 131.43, 131.71, 146.74, 155.35, 156.61, 164.22, 164.98. FAB-MS (NBA/NaI) m/z 433.0215 $(M + H)^+$, $C_{17}H_{12}F_3O_8S$ requires 433.0205.

Representative Procedure for the Palladium-Catalyzed Cross-Coupling of 8 with Substituted Anilines. The aryl coupling procedure reported by Buchwald and Hartwig was used to prepare compounds **9**−**23**. A flame-dried 10 mm by 13 cm borosilicate test tube, equipped with a stir bar and capped with a septum, was charged with **8** (140 mg, 0.324 mmol), palladium dibenzylidene acetone, $Pd_2(dba)_3$ (15 mg, 0.016 mmol), (±)-binap (15 mg, 0.024 mmol), Cs_2CO_3 (147 mg, 0.456 mmol), and aniline (32 μL, 0.356 mmol). Upon addition of all reagents the tube was purged with argon for 10 min. Anhydrous toluene (2.4 mL) was then added through the septum, and the reaction mixture was heated to 100 °C for 36 h in an oil bath. The reaction mixture was filtered through Celite, and the solvent was removed from the filtrate under reduced pressure. The resulting dark oil was purified by flash chromatography over silica (30% EtOAc in hexanes) to afford biarylamine **17** as a white solid (0.12 g, 68%). Refer to the Supporting Information for specific synthetic details and characterization data for compounds **10**−**23** analogous to that reported for **9** below.

1-Phenylaminodibenzofuran-4,6-dicarboxylic Acid Dimethyl Ester (9). ^{1}H NMR (500 MHz, $CDCl_3$) δ 4.06 (s, 3H), 4.11 (s, 3H), 6.49 (br s, 1H), 7.11 (d, J = 8.6 Hz, 1H), 7.14−7.20 (m, 1H), 7.28−7.31 (m, 2H), 7.38−7.44 (m, 3H), 7.97 (dd, J = 1.3, 7.7 Hz, 1H), 8.03 (d, J = 8.6 Hz, 1H), 8.12 (dd, J = 1.3, 7.7 Hz, 1H); ^{13}C NMR (125 MHz, $CDCl_3$) δ 52.05, 52.50, 107.37, 108.82, 112.23, 115.43, 121.30, 122.90, 124.07, 124.31, 125.33, 128.63, 129.73, 131.88, 140.28, 144.58, 154.40, 156.81, 165.16; MALDI-FTMS 375.1094 m/z $(M^{\bullet})^+$, $C_{22}H_{17}NO_5$ requires 375.1106.

Representative Procedure for the Copper-Mediated Cross-Coupling of Phenol 7 with Substituted Phenylboronic Acids To Afford 1-Phenoxydibenzofurans 39−43. The biaryl ether coupling was directly adapted from the procedures reported by Chan and Evans. A 20-mL scintillation vial equipped with a magnetic stir bar was charged with phenol **7** (150 mg, 0.50 mmol), copper (II) acetate (91 mg, 0.5 mmol), freshly activated 4 Å molecular sieves (~250 mg), and phenylboronic acid (180 mg, 1.5 mmol). Dichloromethane (5 mL) was added followed by pyridine (201 μL, 2.5 mmol), resulting in an aqua-colored suspension. The cap was very loosely applied such that the reaction suspension was partly open to the atmosphere. The reaction was monitored by TLC. After completion, the reaction mixture was adsorbed onto ~6 g of silica gel, adding silica gel to the reaction mixture and then removing the solvent under reduced pressure. Chromatography (30% EtOAc in hexanes) of the reaction mixture over silica afforded biaryl ether **39** as a white solid (29 mg, 15%). Refer to the Supporting Information for specific synthetic details and characterization data for compounds **40**−**43** analogous to that reported for **39** below.

1-Phenoxydibenzofuran-4,6-dicarboxylic Acid Dimethyl Ester (39). ^{1}H NMR (500 MHz, $CDCl_3$) δ 4.09 (s, 3H), 4.13 (s, 3H), 6.73 (d, J = 8.8 Hz, 1H), 7.25−7.31 (m, 3H), 7.42−7.50 (m, 3H), 8.07 (d, J = 8.8 Hz, 1H), 8.18 (dd, J = 1.1, 7.7 Hz, 1H), 8.38 (dd, J = 1.1, 7.7 Hz, 1H); ^{13}C NMR (125 MHz, $CDCl_3$) δ 52.29, 52.46, 109.42, 110.02, 114.93, 115.28, 120.52, 123.31, 123.87, 125.34, 127.79, 129.51, 130.26, 131.56, 154.56, 154.73, 156.75, 157.55, 164.88, 165.20; MALDI-FTMS 399.0825 m/z $(M + Na)^+$, $C_{22}H_{16}O_6Na$ requires 399.0839.

Representative Procedure for the Palladium-Catalyzed Cross-Coupling of Triflate 8 with Substituted Phenylboronic Acids. A flame-dried 10 mm by 13 cm test tube, equipped with a stir bar and capped with a septum, was charged with **8** (100 mg, 0.23 mmol), $Pd(PPh_3)_4$ (14 mg, 0.01 mmol), LiCl (29 mg, 0.69 mmol), Na_2CO_3 (300 μL of a 2 M aqueous solution), and toluene (3 mL). Phenylboronic acid (43 mg, 0.35 mmol) was dissolved in EtOH (0.5 mL) and added to the reaction mixture. MeOH replaced EtOH in this procedure for all other compounds because transesterification was observed; therefore compound **49** was isolated as the diethyl ester and all other compounds as dimethyl esters. After the reagents were added, the tube was purged with argon and the reaction mixture heated to 100 °C for 12 h in an oil bath. The reaction mixture was then filtered through Celite. The solvent was removed under reduced pressure from the filtrate, and the resulting dark residue was purified by flash chromatography over silica to afford biaryl **49** as a white solid (52 mg, 63%). Refer to the Supporting Information for specific synthetic details and characterization data for compounds **50**−**59** analogous to that reported for **49** below.

1-Phenyldibenzofuran-4,6-dicarboxylic Acid Diethyl Ester (49). ^{1}H NMR (400 MHz, $CDCl_3$) δ 1.52−1.57 (m, 6H), 4.53−4.62 (m, 4H), 7.20 (t, J = 7.9 Hz, 1H), 7.33 (d, J = 7.9 Hz, 1H), 7.50−7.62 (m, 5H), 7.64 (dd, J = 1.4, 7.8 Hz, 1H), 8.09 (dd, J = 1.3, 7.7 Hz, 1H), 8.18 (d, J = 7.9 Hz, 1H); ^{13}C NMR (100 MHz, $CDCl_3$) δ 14.38, 14.41, 61.38, 114.82, 115.98, 122.45, 124.29, 124.59, 126.70, 127.08, 128.62, 128.73, 128.78, 129.70, 138.71, 142.39, 164.58, 164.61; MALDI-FTMS 411.1197 m/z $(M + Na)^+$, $C_{24}H_{20}O_5Na$ requires 411.1203.

Representative Procedure for Ester Hydrolysis To Afford Final Inhibitors 24−38, 44−48, and 60−70. Methyl ester **9** (25 mg, 0.067 mmol) was saponified in THF: MeOH: H_2O (3:1:1, 1 mL) in a 20-mL scintillation vial equipped with a stir bar. $LiOH{\cdot}H_2O$ (22 mg, 0.53 mmol) was added to the suspension, and the reaction was allowed to stir until completion (typically 4 h) as determined by TLC or analytical reverse-phase HPLC monitoring. The reaction mixture was diluted with

(60) Echavarren, A. M.; Stille, J. K. *J. Am. Chem. Soc.* **1987**, *109*, 5478−5486.

brine (2 mL) and acidified to pH 2 with 1 M HCl (pH paper), resulting in a biphasic solution. The upper layer (THF) was removed, and the aqueous layer was extracted with THF (3 × 3 mL). The combined organic layers were dried with $MgSO_4$ and then concentrated under reduced pressure to afford diacid **24** as a white solid (21 mg, 92%). Refer to the Supporting Information for specific synthetic details and characterization data for compounds **25**−**38**, **44**−**48**, and **60**−**70** analogous to the data reported for **24** below.

1-Phenylaminodibenzofuran-4,6-dicarboxylic Acid (24). ^{1}H NMR (600 MHz, THF-d_8) δ 7.00−7.04 (m, 1H), 7.12 (d, J = 8.6 Hz, 1H), 7.22 (d, J = 7.7 Hz, 1H), 7.29−7.36 (m, 3H), 7.88 (s, br, 1H), 7.98 (d, J = 8.5 Hz, 1H), 8.03 (d, J = 7.5 Hz, 1H), 8.15 (d, J = 7.7 Hz, 1H); ^{13}C NMR (150 MHz, THF-d_8) δ 108.51, 110.04, 113.70, 116.30, 120.73, 122.36, 122.84, 124.78, 126.43, 128.80, 129.51, 131.95, 142.47, 144.86, 154.87, 157.36, 164.96, 165.24; MALDI-FTMS 347.0794 m/z $(M^{\bullet})^+$, $C_{20}H_{13}NO_5$ requires 347.0788.

Acknowledgment. We thank the National Institutes Health (DK 46335), the W. M. Keck Foundation, the Skaggs Institute for Chemical Biology, the Lita Annenberg Hazen Foundation, and the ACS Organic Division, pre-doctoral fellowship (H.M.P.) for financial support. The technical expertise of Dr. Hossein Razavi and Michael Simpson is also greatly appreciated.

Supporting Information Available: Experimental data for compounds formed from the three key reactions, fibril formation results for the dibenzofuran inhibitors lacking C1 appended groups, 7.2 μM fibril formation results for all inhibitors. This material is available free of charge via the Internet at http://pubs.acs.org.

JA044351F